

Activity-Dependent Adjustments of the Inhibitory Network in the Olfactory Bulb following Early Postnatal Deprivation

Armen Saghatelian,¹ Pascal Roux,²
Michele Migliore,^{3,5} Christelle Rochefort,^{1,6}
David Desmaisons,¹ Pierre Charneau,⁴
Gordon M. Shepherd,³ and Pierre-Marie Lledo^{1,*}

¹Laboratory of Perception and Memory

Pasteur Institute

Centre National de la Recherche

Scientifique (URA 2182)

75015 Paris Cedex

France

²Platform of Dynamic Imaging

Pasteur Institute

25 rue du Dr. Roux

75015 Paris Cedex

France

³Department of Neurobiology

Yale Medical School

333 Cedar Street

New Haven, Connecticut 06510

⁴Laboratory of Molecular Virology and Vectorology

Pasteur Institute

28 rue du Dr. Roux

75724 Paris

France

Summary

The first-order sensory relay for olfactory processing, the main olfactory bulb (MOB), retains the ability to acquire new interneurons throughout life. It is therefore a particularly appropriate region for studying the role of experience in sculpting neuronal networks. We found that nostril closure decreased the number of newborn granule cells in the MOB, the complexity of their dendritic arborization, and their spine density, without affecting the preexisting population of granule cells. Accordingly, the frequency of miniature synaptic inhibitory events received by mitral cells was reduced. However, due to a compensatory increase in newborn granule cell excitability, action potential-dependent GABA release was dramatically enhanced, thus counteracting the reduction in spine density and leading to an unaltered synchronization of mitral cell firing activity. Together, this study reveals a unique form of adaptive response brought about exclusively by the cohort of newborn cells and used to maintain normal functioning of the MOB.

Introduction

The functional properties of networks in the brain can be adjusted to constantly changing developmental and

environmental conditions. The continuous postnatal supply of newborn inhibitory interneurons to the main olfactory bulb (MOB) offers an ideal system to study neuronal adjustment regulated by sensory experiences. Progenitor cells originating from the subventricular zone (SVZ) of the lateral ventricle first migrate tangentially to the MOB, by way of the rostral migratory stream (RMS), and then migrate radially within MOB before they differentiate into local interneurons (Luskin, 1993; Lois and Alvarez-Buylla, 1994). It has been hypothesized that postnatal neurogenesis is controlled by levels of sensory activity (Frazier-Cierpial and Brunjes, 1989; Corotto et al., 1994; Kirschenbaum et al., 1999; Saghatelian et al., 2003; Lledo et al., 2004). Hence, although proliferation and tangential migration of neuroblasts are not affected by bulbar removal (Kirschenbaum et al., 1999) or nostril occlusion (Frazier-Cierpial and Brunjes, 1989; but see also Corotto et al., 1994), decreased radial migration (Saghatelian et al., 2004) and increased neuronal death (Frazier-Cierpial and Brunjes, 1989; Najbauer and Leon, 1995; Fiske and Brunjes, 2001) have been both reported in deprived bulbs. In contrast, odor enrichment increases the number of newborn granule cells and improves olfactory memory (Rochefort et al., 2002). It is noteworthy that granule cells provide inhibition onto output bulbar neurons (i.e., mitral/tufted cells) that is responsible for their oscillatory synchronization (Friedman and Strowbridge, 2003; Lagier et al., 2004), and thus for information processing (Laurent et al., 2001; Lledo and Gheusi, 2003). Yet, it is unknown whether the newborn interneurons actively participate in the oscillatory synchronization of principal cells, or what their functional implications are for overall bulbar activity. In principle, any variation in the number and/or the morphology of newborn neurons might disrupt the activity of bulbar output neurons and thus information processing. A small number of studies have attempted to address these issues with unexpected results. For instance, measurements of the paired-pulse inhibition of evoked potentials following stimulation of lateral olfactory tract in control and odor-deprived bulbs demonstrated that a reduced number of newborn interneurons surprisingly increased the level of inhibition received by mitral cells (Wilson et al., 1990; Wilson and Wood, 1992; Wilson, 1995).

Here, using unilateral odor deprivation in combination with quantitative immunohistological, biphoton, and electrophysiological analyses, we explore the functional consequences of reduced neurogenesis on the activity of the bulbar network. We show that sensory deprivation specifically reduces the dendritic length, spine density, and total number of newborn but not of preexisting granule cells. As a consequence, action potential- and glutamate-independent GABA release is impaired. Interestingly, however, sensory deprivation also strengthens action potential-dependent GABA release, since newborn granule cells were more excitable. Such a compensatory effect preserves the overall inhibition and thus the spatiotemporal synchronization of output neurons. Together, this study demonstrates

*Correspondence: pmlledo@pasteur.fr

⁵Permanent address: Institute of Biophysics, National Research Council, Palermo, Italy.

⁶Present address: Max-Planck Institute for Molecular Genetics, 14195 Berlin, Germany.

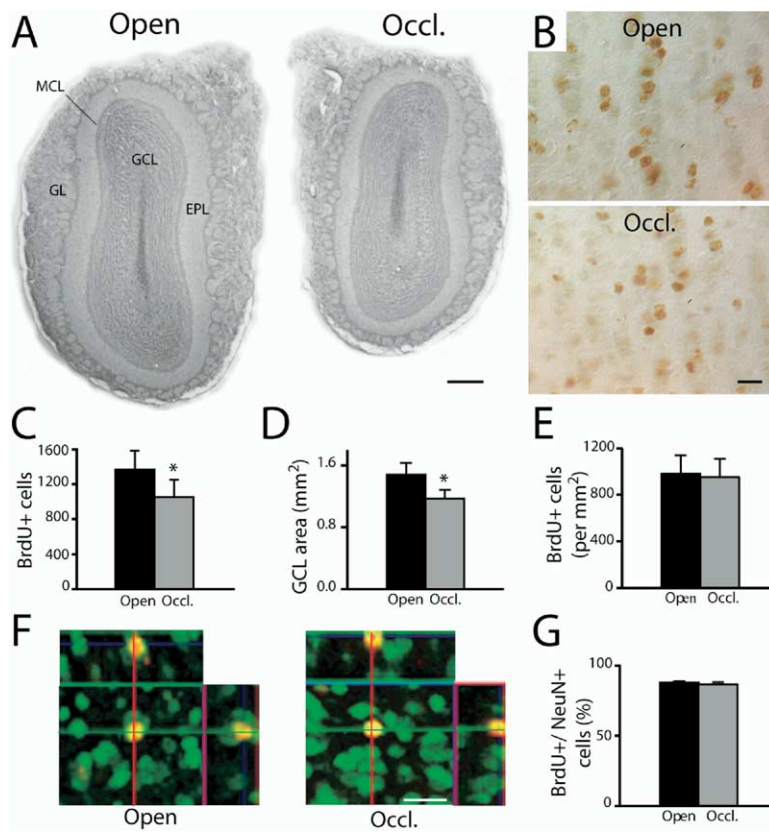


Figure 1. Unilateral Olfactory Deprivation Reduces the Number of BrdU-Positive Cells in the MOB

(A) Photomicrographs of coronal sections displaying the different layers of the MOB. Note the size difference between the control (Open) and the occluded (Occl.) bulb sections of the same animal taken at the same rostrocaudal position. (B) BrdU-positive cells in the granule cell layer of the control (Open) and odor-deprived (Occl.) bulbs. (C and D) Decrease in the number of newly born neurons (C) and GCL area (D) following odor deprivation. (E) Density of BrdU-labeled cells in the control and odor-deprived bulbs. BrdU counting was performed 21 days following BrdU injections and 33 days following unilateral nostril occlusion. * $p < 0.05$ with a Student's t test. (F) Confocal 3D reconstruction of BrdU⁺ cells (red) in control (left panel) and odor-deprived (right panel) bulbs stained for the neuronal marker NeuN (green). Reconstructed orthogonal projections are presented as viewed in the x-z (top) and y-z (right) planes. (G) Percentage of BrdU⁺ cells double labeled for NeuN in control (Open) and odor-deprived (Occl.) bulbs. Scale bars, 300 μm in (A), 10 μm in (B) and (F). GL, glomerular layer; EPL, external plexiform layer; MCL, mitral cell layer; GCL, granule cell layer.

that the cohort of newborn granule cells brings to the MOB unique adaptive properties and thus upholds the function of the neuronal network in response to the ever-changing olfactory world.

Results

Odor Deprivation Reduces the Number of Newborn Granule Cells

To investigate whether sensory activity regulates the number of newborn interneurons, we quantified their abundance in the MOB following unilateral odor deprivation using 5-bromo-2'-deoxyuridine (BrdU) as a cell division marker. In agreement with previous results (Brunjes, 1994), 30–40 days of odor deprivation starting at postnatal days 4–5 (P4–P5) reduces MOB size (Figure 1A). It also decreases the number of newborn cells labeled at P16 and counted 21 days later in the granule cell layer (GCL) (1370 ± 216 and 1053 ± 157 for control and odor-deprived bulbs, respectively; $n = 6$; $p < 0.01$, paired Student's t test; Figures 1B and 1C). The reduced number of newborn cells was not due to a decrease in proliferation rate, since quantification of BrdU⁺ profiles in the SVZ-RMS area, 4 hr after BrdU injections, did not reveal any significant difference between control and occluded bulbs (respectively, 450 ± 25 and 433 ± 18 cells; $n = 4$; $p > 0.05$, paired Student's t test). The reduction in newborn cell number was specific to the GCL, as no change was found in the glomerular layer in terms of number (controls, 68.1 ± 15 ; oc-

cluded, 59.1 ± 13 ; $n = 4$; $p > 0.05$, paired Student's t test) and density (controls, 95.5 ± 26.7 cells/ mm^2 and occluded, 98 ± 20.8 cells/ mm^2 ; $n = 4$; $p > 0.05$, paired Student's t test) of newborn periglomerular neurons. The area of GCL was also reduced by odor deprivation (1.17 ± 0.11 mm^2 in occluded and 1.48 ± 0.15 mm^2 in control bulbs; $n = 6$; $p < 0.01$, paired Student's t test; Figure 1D). This meant that, despite the decrease in cell number, occlusion produced no change in the density of newborn granule cells (controls, 984 ± 155 cells/ mm^2 ; deprived bulbs, 952 ± 156 cells/ mm^2 ; $n = 6$; $p > 0.05$, paired Student's t test; Figure 1E). To determine whether sensory deprivation also alters cell fate, we estimated the proportion of cells double labeled for BrdU and the neuronal marker NeuN (Figure 1F). Orthogonal projections through 3D reconstructed BrdU⁺ cells revealed that in both conditions about 85% of newborn cells were neurons ($n = 400$ and 380 BrdU⁺ cells for control and odor-deprived bulbs, respectively, from four animals; $p > 0.05$, paired Student's t test; Figure 1G).

It has been demonstrated that a reduced number of newborn cells following sensory deprivation is mainly due to their decreased survival rate after they have reached and positioned themselves in the GCL (Petreanu and Alvarez-Buylla, 2002), processes that take about 2 weeks in both newborn and adult rats (Luskin, 1993; Winner et al., 2002). Thus, it is likely that the reduction in number of newborn granule cells observed in our experiments takes place during the last 7–10 days of the BrdU postinjection period. Bearing in mind

this critical time period required for the survival of newborn granule cells, and also observations demonstrating high local production of granule cells in the MOB during the first postnatal week (Hinds, 1968), we investigated whether sensory deprivation also affects the preexisting population of granule cells. When the resident population of granule cells produced locally in the MOB was labeled by a single BrdU injection in P2 pups, sensory deprivation performed at P4 failed to reduce their number 7 days later (390.9 ± 43.4 and 397.3 ± 46.6 for control and odor-deprived bulbs, respectively; $n = 3$; $p > 0.05$, paired Student's *t* test). Together, these results demonstrate that odor deprivation specifically reduced the number of newborn neurons located in the GCL, but not those positioned in the glomerular layer, without changing the proliferation rate or the GCL cell density.

Odor Deprivation Affects the Maturation of Newborn Granule Cells

Although the density of newborn granule cells remains unchanged in deprived bulbs, it is plausible that sensory deprivation alters their morphology and/or their spine density. To explore this, neuronal precursors were labeled in the SVZ using a GFP-expressing lentiviral vector, and newborn neurons were morphologically analyzed in the GCL, 25 days after the vector injection and following 45 days of odor deprivation. Interestingly, newborn granule cells displayed a less complex morphology in occluded bulbs as compared to controls (Figure 2A). Odor deprivation drastically reduced the length of the apical dendrite from the soma to the first point of ramification (e.g., the primary dendrite) (controls, $168.1 \pm 10.1 \mu\text{m}$; occluded bulbs, $101.2 \pm 7.9 \mu\text{m}$; $n = 40$ cells per condition from three animals; $p < 0.01$, unpaired Student's *t* test; Figure 2B). The total length of the dendritic tree was also significantly reduced (controls, $332.6 \pm 24.9 \mu\text{m}$; occluded bulbs, $245.4 \pm 24.5 \mu\text{m}$; $n = 40$ cells per condition from three animals; $p < 0.05$, unpaired Student's *t* test; Figure 2B). Since odor deprivation decreases the overall size of the MOB, the reduced length of the dendritic arborization might simply arise from general shrinkage of the GCL and the external plexiform layer (EPL). To explore this possibility, we normalized the length of the primary dendrite as well as the entire dendritic tree of newborn granule cells with respect to the 25% reduction in the size of the GCL and the EPL measured in the same slices. Interestingly, whereas the length of the primary dendrite was still significantly smaller in deprived bulbs (controls, $168.1 \pm 10.1 \mu\text{m}$; occluded bulbs, $126.5 \pm 9.9 \mu\text{m}$; $n = 40$ cells per condition from three animals; $p < 0.05$, unpaired Student's *t* test), no difference in the length of the dendritic tree was observed (controls, $332.6 \pm 24.9 \mu\text{m}$; occluded bulbs, $306.7 \pm 30.6 \mu\text{m}$; $n = 40$ cells per condition from three animals; $p > 0.05$, unpaired Student's *t* test). This finding indicates that the reduction in the length of dendritic arborizations of newborn granule cells cannot be solely explained by overall shrinkage of MOB. When we performed a similar analysis on mitral cells labeled with protein gene product 9.5 (PGP 9.5) antibody (Nakajima et al., 1998), a 30% reduction in the length of mitral cells' primary dendrite in the deprived bulb (controls, $323.8 \pm 15.8 \mu\text{m}$; oc-

cluded bulbs, $261.5 \pm 21.1 \mu\text{m}$; $n = 15$ cells per condition from two animals; $p < 0.05$, unpaired Student's *t* test) was accompanied by a 30% reduction in the size of EPL (controls, $2.75 \pm 0.01 \mu\text{m}$; occluded bulbs, $2.11 \pm 0.01 \mu\text{m}$; $n = 15$ cells per condition from two animals; $p < 0.05$, unpaired Student's *t* test). Interestingly, newborn granule cells in the odor-deprived bulb also demonstrate a 2-fold reduction in spine density (from 0.20 ± 0.01 spine/ μm in controls to 0.11 ± 0.007 spines/ μm in occluded bulbs, respectively; $n = 40$ cells from three animals; $p < 0.01$, unpaired Student's *t* test; Figures 2C and 2D). These results demonstrate that sensory activity is essential for the normal growth of newborn granule cell dendrites, and for normal newborn cell spine density.

To explore whether sensory deprivation also affects the dendritic architecture and spine density of the preexisting population of granule cells, we injected Dil directly to the P3 MOB and analyzed cell morphology 10 days later. This time was chosen because the effect of sensory deprivation on newborn granule cell architecture and spine density is likely taking place during the last 7–10 days of GFP vector postinjection, when labeled precursors finish their migration and positioning in the GCL. Additionally, it is conceivable that granule cell progenitors born in the SVZ and RMS after sensory deprivation performed at P4 are not yet incorporated into the MOB network, thus providing a more or less homogenous population of resident granule cells at this time point. The length of the primary dendrite as well as the entire dendritic tree was very similar for this preexisting granule cell population in control and occluded bulbs (controls, $128.5 \pm 19 \mu\text{m}$ and $129.4 \pm 24.3 \mu\text{m}$; occluded bulbs, $126.5 \pm 7.4 \mu\text{m}$ and $114.6 \pm 9.7 \mu\text{m}$; $n = 12$ cells per condition from two animals; $p > 0.05$, unpaired Student's *t* test; Figures 2E and 2F). Similarly, no difference in the spine/filopodia density of Dil-labeled granule cells was observed following sensory deprivation (0.14 ± 0.01 spine/ μm and 0.13 ± 0.01 spines/ μm in the control and occluded bulbs, respectively; $n = 30$ – 40 cells from two animals; $p > 0.05$, unpaired Student's *t* test; Figures 2G and 2H). These results strongly suggest that sensory deprivation specifically affects the morphology and spine density of the newborn, but not the preexisting, granule cell population.

Consequences of Odor Deprivation on Spontaneous Synaptic Transmission in the MOB

To investigate the functional consequences of a reduced spinogenesis in newborn granule cells, we employed electrophysiological recordings on their target output neurons: the mitral cells. Neither their general cell morphology (assessed by Dil labeling) nor their intrinsic membrane properties assessed by intracellular recordings (data not shown) were altered by nostril occlusion. We then recorded spontaneous synaptic activity impinging on mitral cells. These neurons receive inhibitory inputs from granule cells via dendrodendritic reciprocal synapses, consisting of an excitatory mitral-to-granule cell synapse directly adjacent to an inhibitory granule-to-mitral cell synapse (Price and Powell, 1970). It has been demonstrated that GABA release is

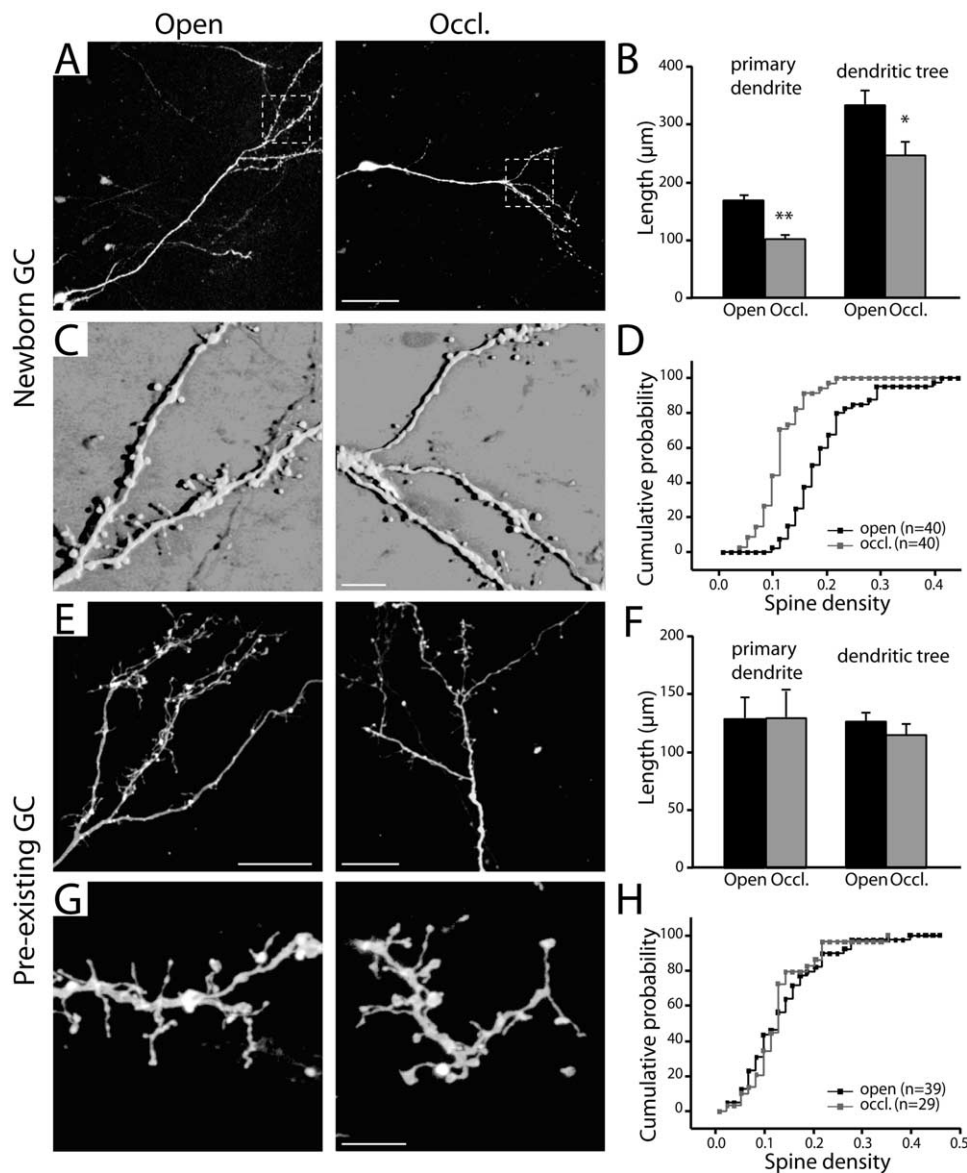


Figure 2. Sensory Deprivation Reduces the Dendritic Length and Spine Density of Newly Generated Granule Cells

(A) Images of GFP-labeled newborn granule cells in a control (Open) and odor-deprived (Occl.) bulb. Note the less complex morphology of newborn cells following odor deprivation.

(B) The lengths of the primary dendrite and total dendritic tree of newborn granule cells in the control and odor-deprived bulbs. Data are presented as means \pm SEM. * and ** indicate significant differences of $p < 0.05$ and $p < 0.01$, respectively.

(C) High-magnification images of the dendritic trees of newborn granule cells in the control (Open) and odor-deprived (Occl.) bulbs. Note reduced spine density for newborn granule cells in the odor-deprived bulb.

(D) Cumulative distribution of spine density of newborn granule cells in the control (open; black line) and odor-deprived (occl.; gray line) bulbs.

(E) Images of Dil-labeled preexisting granule cell dendrites in the control (Open) and odor-deprived (Occl.) bulb.

(F) The lengths of primary dendrite and total dendritic tree of the Dil-labeled resident population of granule cells in the control and odor-deprived bulbs. Data are presented as means \pm SEM.

(G) High-magnification images of the dendritic tree of the preexisting population of granule cells in the control (Open) and odor-deprived (Occl.) bulbs.

(H) Cumulative distribution of the spine density of newborn granule cells in the control (Open; black line) and odor-deprived (Occl.; gray line) bulbs. Scale bars, 50 μ m in (A), 25 μ m in (E), 10 μ m in (C), and 7 μ m in (G).

triggered by activation of glutamatergic receptors located on granule cell spines (Isaacson and Strowbridge, 1998; Schoppa et al., 1998; Chen et al., 2000; Halabisky et al., 2000; Isaacson, 2001). In addition, spontaneous granule-to-mitral cell GABAergic inhibition also occurs in the absence of glutamatergic recep-

tor activation through both action potential-dependent and -independent GABA release (Castillo et al., 1999). We compared the contribution of each of the three components to the GABAergic inhibition between control and odor-deprived bulbs.

Application of the broad-spectrum ionotropic gluta-

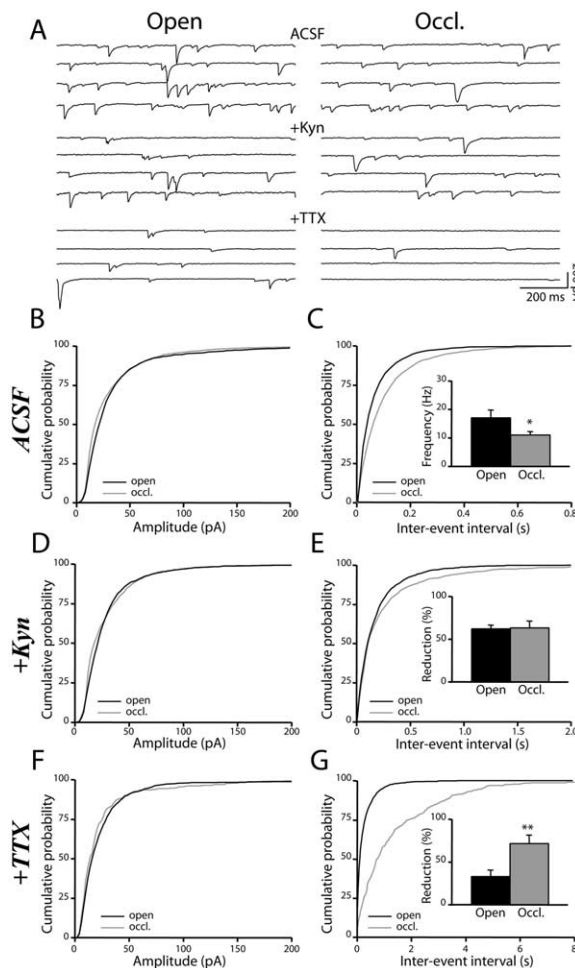


Figure 3. Odor Deprivation Reduces the Frequency of mIPSCs

(A) Individual experiments illustrating spontaneous synaptic responses recorded from mitral cells in control and odor-deprived bulbs. Applications of the glutamatergic receptor antagonist kynureate (Kyn; 5 mM) and the Na⁺ channel blocker tetrodotoxin (TTX; 1 μM) were used to assess the contribution of glutamate- and action potential-induced GABA release, respectively. Note the higher decrease in sIPSC frequency recorded from a mitral cell in an odor-deprived bulb during application of TTX. Cumulative distribution of sPSC amplitudes in the mitral cells of the control (black line) and occluded (gray line) bulbs under control conditions (B) and after application of 5 mM Kyn (D) and 1 μM TTX (F). (C) Cumulative distribution of interevent intervals of sPSCs under control conditions in open (black line) and occluded (gray line) bulbs. Inset shows the mean sPSC frequency recorded from mitral cells in control (17.12 ± 2.68 Hz) and odor-deprived (11.08 ± 1.2 Hz) bulbs (*p < 0.05; Mann-Whitney U test). (E and G) Cumulative distribution of interevent intervals in the control (open; black line) and occluded (occl.; gray line) bulbs during application of Kyn (E) and TTX (G). Insets show the mean reduction of sPSC frequency in the presence of Kyn (E) and TTX (G). Note the significantly stronger reduction in sIPSC frequency in the deprived as compared to the control bulbs following TTX treatment. * and ** indicate significant differences of p < 0.05 and p < 0.01, respectively (Mann-Whitney U test).

matergic antagonist kynureate (Kyn; 5 mM) to control bulb slices strongly decreased the frequency (62.2% ± 4.5% reduction; n = 8; p < 0.001), but not the amplitude (2.4% ± 10.5% reduction; n = 8; p > 0.05), of spontaneous postsynaptic currents (sPSCs) (Figure 3A). Subse-

quent bath application of the Na⁺ channel blocker TTX (1 μM) further reduced the frequency of glutamate-independent spontaneous inhibitory postsynaptic currents (sIPSCs) (33.2 ± 7.3% reduction, n = 8; p < 0.001; Figure 3A). As previously found for mice (Castillo et al., 1999), the frequency of spontaneous synaptic events was more strongly attenuated by Kyn than by TTX (Figure 3A), demonstrating the importance of glutamate-induced GABA release by the tonic form of inhibition. These recordings further demonstrate that mitral cells receive sPSCs driven by glutamate receptor activation and occurring at high frequency, sIPSCs triggered by action potentials and occurring with lower frequency and, finally, inhibitory postsynaptic currents (IPSCs) independent of both glutamate receptor activation and action potentials, here called miniature IPSCs (mIPSCs).

Having isolated the three types of GABAergic events in mitral cells, we then investigated their potential changes following odor deprivation. Similar to the control situation, applications of Kyn and TTX strongly affected the frequency, but not the amplitude, of sPSCs in mitral cells from odor-deprived bulbs (Figure 3A). Interestingly, while frequencies of sPSCs and sIPSCs were only slightly decreased following odor deprivation (Figures 3C and 3E), the reduction of mIPSC frequency was much more severe (Figure 3G). Such a reduction is consistent with our finding of reduced spine density in newborn granule cells and implies that newborn granule cells play an important role in providing a strong inhibition on output neurons. Additionally, a highly significant reduction in the frequency of mIPSCs coupled with only subtle modifications in the frequency of sIPSCs further demonstrates that the contribution of action potential-dependent GABA release might be altered following odor deprivation. Quantifying the percentage reduction in the sIPSC frequency following application of TTX further supported this notion: highly significant changes between control and occluded bulbs were observed following addition of 1 μM TTX (Figure 3G, inset). The mean reduction in sIPSC frequency was 33.2% ± 7.3% for control and 71.6% ± 9.9% for occluded bulbs (n = 8; p < 0.001, Mann-Whitney U test). By contrast, application of Kyn (5 mM) induced a similar reduction of sPSC frequency (62.2% ± 4.5% and 63.5% ± 7.9% reduction in the control and occluded bulbs, respectively; n = 8; Figure 3E, inset). In addition, the amplitude of the three types of GABAergic synaptic events was similar between controls and odor-deprived bulbs (Figures 3B, 3D, and 3F), suggesting that restriction of sensory inputs does not alter postsynaptic GABA_A receptors. Together, these results show that newborn granule cells contribute to the massive inhibitory input to mitral cells and that alterations in the efficiency of this input activate some action potential-dependent compensatory mechanisms.

Bidirectional Modulation of Evoked Synaptic Responses following Nostril Occlusion

To assess whether restriction in the degree of sensory inputs might decrease evoked granule-to-mitral cell responses, mitral cells were transiently depolarized using voltage steps. Release of glutamate induced by depolarizing mitral cells has been shown to excite granule

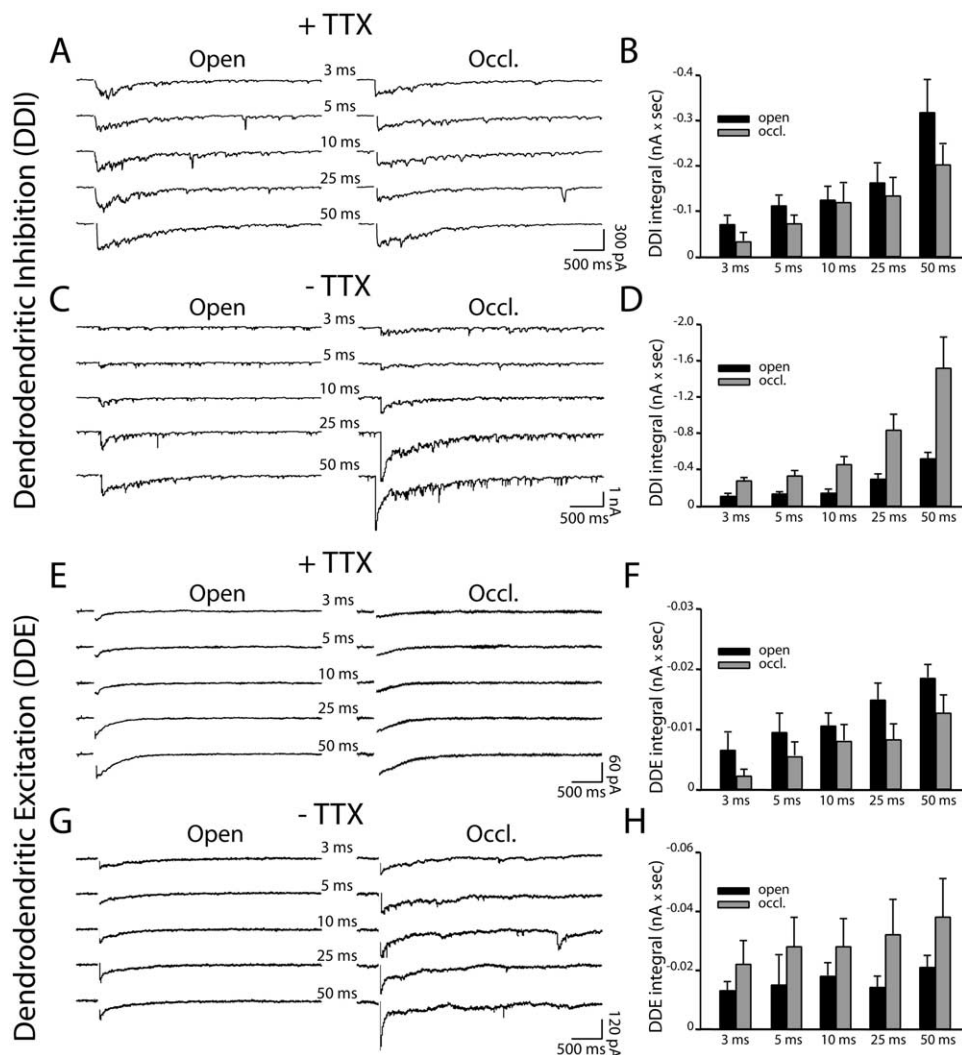


Figure 4. Dendrodendritic Responses in Odor-Deprived Animals

A brief depolarizing step in mitral cells induced dendrodendritic inhibition (DDI) in the control (Open) and odor-deprived (Occl.) bulbs, in the presence (A) and absence (C) of TTX (1 μ M). Numbers above the traces indicate the duration of the depolarizing steps. Note that the charge of DDI was only slightly affected by nostril occlusion in the presence of TTX (B) and was even increased when action potentials were not blocked (D). Black and gray bars represent the values obtained from control ($n = 7$ –10 cells) and odor-deprived ($n = 8$ –11 cells) bulbs, respectively, obtained at different durations of depolarization steps (x axis). Dendrodendritic excitation (DDE) in control (Open) and odor-deprived (Occl.) bulbs under conditions when TTX (1 μ M) was present (E) or absent (G). Note that the integral of DDE in the mitral cells of occluded bulbs is reduced in the absence of TTX (F) and increased in the presence of TTX (H). Black and gray bars represent the values obtained from control ($n = 5$ –7 cells) and odor-deprived ($n = 7$ –8 cells) bulbs, respectively, at different depolarization steps and conditions. Data are means \pm SEM.

cell spines that, in turn, mediate GABAergic dendrodendritic inhibition (DDI) of the mitral cells (Isaacson and Strowbridge, 1998; Chen et al., 2000; Halabisky et al., 2000; Isaacson, 2001). It has been shown that a short depolarization (2–3 ms) recruits voltage-activated Ca^{2+} channels that are required to trigger GABA release. In contrast, longer depolarizations (25–50 ms) induce GABA release that depends on NMDA receptor activation (Halabisky et al., 2000). Thus, we recorded DDI responses at different steps of depolarization and isolated them by subtracting the traces recorded with a specific GABA_A receptor antagonist, bicuculline methiodide (BMI; 40 μ M), from those recorded under

standard conditions. To investigate whether the reduced spine density of newborn granule cells would affect evoked DDI responses, mitral cells were depolarized with increasing voltage step duration in the presence of TTX (1 μ M) (Figures 4A and 4B). In addition, since our recordings of spontaneous synaptic activity suggested increased action potential-dependent GABA release from granule cells of occluded bulb, we also recorded DDI responses in the absence of TTX (Figures 4C and 4D). Interestingly, whereas the integral (Figure 4B) and amplitude (data not shown) of DDI responses recorded with TTX (1 μ M) tended to be smaller in the occluded bulb, the opposite effect was observed when

TTX was omitted. Both integral (Figure 4D) and amplitude (data not shown) were significantly higher in deprived bulbs. These results suggest that the reduced spine density of newborn granule cells also slightly contributes to evoked local inhibitory dendrodendritic responses in the MOB. However, due to the compensatory increase in action potential-dependent GABA release, DDI responses were not reduced, but rather increased, in deprived bulbs, demonstrating an increase in the global inhibition of mitral cells.

Application of BMI left a small component that was further blocked by Kyn (5 mM). This dendrodendritic excitatory (DDE) component represents either autoexcitation of mitral cell dendrites (Isaacson, 1999; Friedman and Strowbridge, 2000; Salin et al., 2001), or activation of excitatory granule-to-mitral cell reciprocal synapses (Didier et al., 2001), or both. As reported for DDI, unilateral nostril occlusion only slightly reduced evoked excitatory responses measured on mitral cells in the presence of TTX (1 μ M) (Figures 4E and 4F), whereas those recorded without TTX were even higher (Figures 4G and 4H). Since we observed opposite effects of sensory deprivation on reciprocal responses recorded with and without TTX, and because the excitability of mitral cells was not altered by odor deprivation, these results favor the involvement of dendrodendritic synapses in the above-mentioned results rather than changes in the glutamate release or autoexcitatory responses. Altogether, these results demonstrate that odor deprivation only slightly influenced local recurrent responses, whereas a compensatory increase in action potential-dependent neurotransmitter release led to stronger lateral synaptic interactions between principal cells following sensory deprivation.

Induced Gamma Oscillations Remain Unchanged in Deprived Bulbs

We have demonstrated the exclusive role of granule cell reciprocal synapses in generating evoked fast oscillations in the MOB (Lagier et al., 2004). To elucidate whether reduced spine density of newborn granule cells and modified dendrodendritic responses following occlusion would affect the synchronization of mitral cells, we recorded local field potentials (LFPs) in control and odor-deprived bulbs following stimulation of the olfactory nerve (Figure 5A). Interestingly enough, all parameters of the induced oscillations in deprived bulbs were similar to those seen in control bulbs (Figures 5B–5D). Nostril occlusion altered neither the amplitude (Figure 5B), nor the duration (920 ± 410 ms in control and 1050 ± 490 ms in occluded bulbs; $n = 6$; Figure 5C), nor the dominant frequency (44 ± 10 Hz and 46 ± 5 Hz in controls and occluded bulbs, respectively; $n = 6$; Figure 5D) of these rhythms. Since LFP oscillations mainly reflect the synchronizing activity of output neurons, we conclude that sensory deprivation does not alter the synchronization of mitral cells. In summary, odor deprivation reduces the spine density of newborn granule cells and therefore the frequency of mIPSCs impinging on mitral cells. Yet GABAergic inhibition and the oscillatory activity of output neurons are preserved. What cellular mechanisms might support this adjustment?

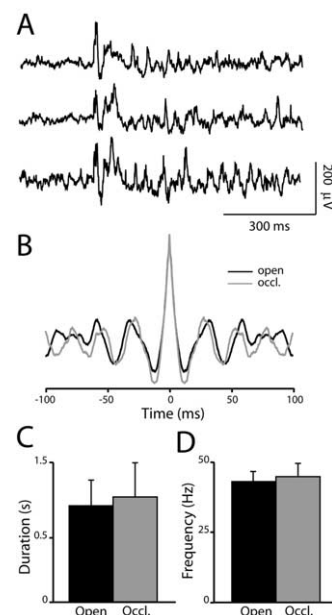


Figure 5. Normal LFP Oscillations in the Odor-Deprived Bulb

(A) Individual experiment demonstrating LFP oscillations measured in the mitral cell layer in response to a brief (100 μ s) olfactory nerve stimulation. (B) Autocorrelation corresponding to the LFP oscillations in control (black line) and odor-deprived (gray line) bulbs. Duration (C) and frequency (D) of LFP oscillations in control ($n = 5$) and occluded ($n = 5$) bulbs. Data are means \pm SEM.

Odor Deprivation Increases the Excitability of Newborn Granule Cells

We explored the mechanism by which elevation of action potential-dependent GABA release might counteract the reduction of spine density in the odor-deprived bulb. To investigate whether increased excitability of granule cells may be involved in this compensation, granule cells were first recorded with the noninvasive cell-attached mode to estimate spontaneous spiking activity. A much higher percentage of spontaneously spiking granule cells was indeed found in occluded bulbs. While only 10% of granule cells ($n = 10$) showed spiking activity in control bulbs, 50% fired in occluded bulbs ($n = 12$). This increased excitability might arise from altered intrinsic electrophysiological properties (Zhang and Linden, 2003) and/or from modified synaptic input to these cells (Turrigiano and Nelson, 2004). We tested initially whether the change in neuronal excitability was correlated with an underlying change in intrinsic currents using the conventional whole-cell technique. We identified several voltage-dependent conductances in granule cells from the control and odor-deprived bulbs by applying a series of depolarizing steps under different pharmacological conditions. First, the resting membrane potential, measured immediately after breaking the patch membrane, was unchanged (occluded bulbs, -59.1 ± 0.7 mV; controls, -58.9 ± 0.7 mV; $n = 20$). We then compared the Na^+ current in control and odor-deprived bulbs. Although the normalized maximum Na^+ current amplitude was not modified (-160 ± 26 pA/pF and -160 ± 42 pA/pF, for control and

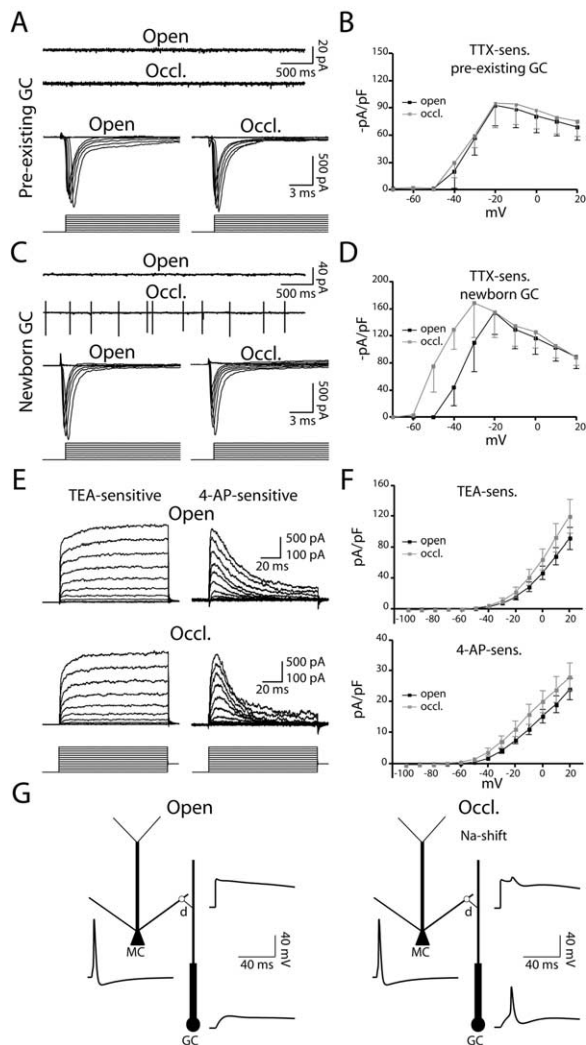


Figure 6. Odor Deprivation Specifically Increases the Spiking Activity of Newborn Granule Cells

(A–D) Individual experiments demonstrating action potential discharges and Na⁺ currents recorded from preexisting (A) and newborn (C) granule cells in the control (Open) and odor-deprived (Occl.) bulbs. Na⁺ currents were induced by depolarizing potentials with increasing steps of 10 mV from –60 mV to +20 mV and were isolated by subtracting the currents recorded before and after TTX (1 μ M). Na⁺ current density in preexisting (B) and newly generated (D) granule cells of control (black line) and odor-deprived (gray line) bulbs. Note the leftward shift in the voltage dependency of Na⁺ current in newborn granule cells following odor deprivation.

(E) Individual experiments showing TEA- and 4-AP-sensitive whole-cell K⁺ currents in the granule cells of control (Open) and odor-deprived (Occl.) bulbs. TEA- and 4-AP-sensitive K⁺ currents were obtained by subtracting the currents recorded before and after 4-AP (5 mM) and TEA (9 mM) applications, respectively. Voltage-dependent currents were induced by increasing depolarization steps of 10 mV, from –100 mV to +20 mV.

(F) Density of TEA- and 4-AP-sensitive currents recorded in control (black line) and odor-deprived (gray line) bulbs. Data are means \pm SEM with 8–16 cells per condition.

(G) Schematic representation of the model under control conditions (left) and following odor deprivation (right). A granule cell (GC) in the odor-deprived bulb was modeled with a 10 mV leftward shift in the voltage-dependent activation of Na⁺ current. Traces below each model are the somatic membrane potential of the mitral cells

occluded bulbs, respectively), its voltage dependency was shifted toward more hyperpolarized membrane potentials in deprived bulbs (data not shown).

These experiments, however, do not allow us to distinguish whether the overall population of granule cells displays increased excitability or whether this effect is more specific to newborn cells. Therefore, we recorded newborn, GFP-labeled, and preexisting granule cells. To assess the excitability and Na⁺ current of the resident population of granule cells, we performed recordings in P15 MOB slices knowing that neurons born in the SVZ and RMS after P4 would not have had enough time to arrive and fully differentiate into granule cells and thus sufficiently contribute to the total granule cell population. Interestingly, when preexisting granule cells were recorded in control and occluded bulbs, not a single cell displayed spontaneous spiking activity in the cell-attached mode ($n = 5$ for each condition; Figure 6A). Similarly, Na⁺ current recorded from the same cells, after rupturing the membrane, showed a similar current density (-92.7 ± 22.6 pA/pF and -95.1 ± 26.7 pA/pF, for control and occluded bulbs, respectively) and voltage dependency (Figures 6A and 6B). In contrast, when we recorded the excitability of GFP⁺ granule cells in P30–P40 animals, dramatic differences between control and deprived bulbs were found. While amongst seven newborn granule cells recorded in the control bulb only one showed spontaneous spiking activity, three out of five new cells in the occluded bulb displayed increased excitability (Figure 6C). Importantly, although no difference in normalized Na⁺ current amplitude was observed in these cells (-154.5 ± 32.4 pA/pF and -168.6 ± 51.2 pA/pF, for control and occluded bulbs, respectively), there was a clear shift of voltage dependency toward more hyperpolarized values in the deprived bulbs (Figure 6D). These results demonstrate that odor deprivation specifically increases the excitability of newborn granule cells via a leftward shift in the voltage dependency of Na⁺ current activation.

Granule cells also display prominent transient fast inactivating A-type and steady-state K⁺ currents (Schoppa and Westbrook, 1999) that control cell excitability (Schrader et al., 2002). These currents were isolated using either 4-aminopyridine (4-AP; 5 mM) or tetraethylammonium chloride (TEA; 9 mM), to block A-type or delayed rectified K⁺ channels, respectively (Figure 6E). No significant change in the current density (Figure 6F) or in the activation/inactivation properties of these channels (data not shown) was observed following odor deprivation.

Finally, we wondered whether the 10 mV leftward shift in the voltage dependency of Na⁺ current activation would be sufficient to increase the excitability of newborn granule cells following sensory deprivation. To assess this possibility, we used a simple model based on one mitral cell and one granule cell connected together (Figure 6G). In standard conditions (Figure 6G,

(MC), and the membrane potential of the terminal dendritic tips (d) and soma (GC) of the granule cell. Note the appearance of the somatic action potential in the granule cell following odor deprivation.

left), a single action potential was elicited in the mitral cell with a short (2 nA, 2 ms) somatic current pulse. Action potential propagation in the mitral cell secondary dendrites activated an excitatory postsynaptic potential (EPSP) on the corresponding small oblique branch of the granule cell. The consequent depolarization then propagated to the entire dendritic tree, but the overall somatic depolarization, however, was not sufficient to elicit an action potential at the soma. To mimic the experimental findings on odor deprivation, the same stimulation protocol was repeated after a 10 mV voltage dependency shift toward more hyperpolarized membrane potentials in the deprived bulb (Figure 6G, right). Interestingly, the EPSP-triggered depolarization was now able to induce sufficient depolarization at the soma of granule cells to trigger action potentials (compare GC traces in Figure 6G), indicating that a 10 mV leftward shift in the activation of Na⁺ current is sufficient to support increased excitability of newborn cells following odor deprivation.

To assess whether altered excitatory/inhibitory synaptic inputs to granule cells might also act in concert with this intrinsic change, we recorded spontaneous synaptic events from granule cells. The global spontaneous synaptic activity received by granule cells in occluded bulbs was undistinguishable from that of controls (amplitude, -17 ± 2.5 pA and -16.4 ± 1.4 pA, in controls and occluded bulbs, respectively; $n = 8$; frequency, 3.35 ± 0.9 Hz and 3.3 ± 0.5 Hz, in controls and occluded bulbs, respectively; $n = 8$; Figures 7A and 7B). However, following application of Kyn, the frequency of sIPSCs measured in granule cells from occluded bulbs was lower when compared to controls (Figures 7C and 7D). Similarly, the percentage of Kyn-induced frequency reduction tended to be higher in odor-deprived bulbs (respectively, $35.9\% \pm 13.2\%$ and $54.2\% \pm 7.7\%$ in controls and occluded bulbs; $n = 8$; $p > 0.05$, Mann-Whitney U test; Figure 7D, inset). Addition of TTX further decreases the frequency of sIPSCs in control and occluded bulbs (Figures 7E and 7F), with a slightly stronger, albeit nonsignificant, effect in the odor-deprived granule cells ($15.1\% \pm 8.4\%$ and $29.9\% \pm 6.6\%$ of reduction in the sIPSCs' frequency from controls and occluded bulbs, respectively; $n = 8$; $p > 0.05$, Mann-Whitney U test; Figure 7F, inset). No change could be seen in the amplitude of sIPSCs (control bulbs, -14 ± 2.2 pA; occluded bulbs, -11.5 ± 1 pA; $n = 8$) or in the amplitude of mIPSCs (control bulbs, -13.5 ± 2.4 pA and occluded bulbs, -12.1 ± 1.1 pA; $n = 8$).

In summary, these recordings demonstrate that odor deprivation increases the excitability of newborn granule cells via a leftward shift in the voltage dependency of Na⁺ current and via affected synaptic inputs impinging on granule cells. Increasing the excitability of newborn granule cells following deprivation might represent a homeostatic compensatory mechanism by which the functional level of the neuronal network remains constant in spite of reduced spine density.

Discussion

We have shown that sensory deprivation reduces the number, the dendritic length, and the spine density of

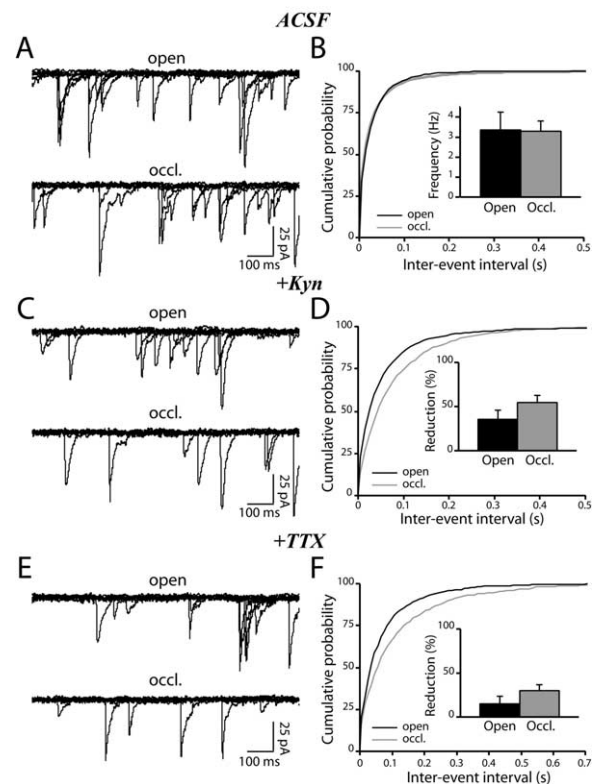


Figure 7. Odor Deprivation Affects the Excitatory-Inhibitory Balance of Granule Cells

Individual experiments illustrating sIPSCs (A), sIPSCs (C), and mIPSCs (E) recorded from granule cells in control (Open) and odor-deprived (Occl.) bulbs. sIPSCs were isolated by adding to the bath medium 5 mM Kyn, whereas mIPSCs were isolated by adding 1 μ M TTX. Note the decreased frequency of sIPSCs and mIPSCs recorded from the granule cell in the occluded bulb. Cumulative inter-event interval distributions of sIPSCs (B), sIPSCs (D), and mIPSCs (F) recorded from granule cells in control (black line; $n = 7$) and occluded (gray line; $n = 8$) bulbs. Insets show the mean frequency of sIPSCs (B), as well as a reduction in the frequency of spontaneous activity following applications of Kyn (D) and TTX (F). Data are means \pm SEM.

newborn granule cells in the MOB. In addition, the frequency but not the amplitude of mIPSCs impinging onto mitral cells is strongly reduced in deprived bulbs. Despite this reduction, the overall inhibitory input onto mitral cells and their synchronization remain unchanged, due to compensatory mechanisms that depend on action potentials. Underlying this adaptation is an increase in the intrinsic excitability of newborn granule cells, which is brought about by changes in the voltage dependency of Na⁺ currents, possibly to offset a reduction in mIPSC frequency. Together, this study highlights an unexpected degree of homeostatic regulation that depends on the level of sensory inputs, which is brought about exclusively by the population of newborn granule cells and is used to keep the bulbar neuronal network within a constant operating range.

The Role of Sensory Activity in Bulbar Neurogenesis
It is widely accepted that the adult brain can respond with morphofunctional changes to environmental and/

or internal challenges. In the olfactory system, odor deprivation affects mainly the granule cell population without any major effects on other neuronal types (Corotto et al., 1994). No change has been found in mitral cells (Benson et al., 1984) or in the branching of their dendrites (Matsutani and Yamamoto, 2000 and present study). In line with this, anosmic mice that have a targeted deletion of a subunit of the olfactory cyclic nucleotide-gated channel (OCNC-1) still form precise synaptic connections that are grossly unaltered (Baker et al., 1999; Lin et al., 2000). This suggests that both targeting of sensory neuron projections into the MOB and refinement of mitral cell dendrites are controlled by genetically encoded spatial cues. However, in animals heterozygous for the OCNC-1 channel gene, Zhao and Reed (2001) have demonstrated that mutant, but not wild-type, neurons in the olfactory epithelium become slowly depleted with time. Additionally, it has been shown recently that odorant stimulation leads to an increased survival of sensory neurons (Watt et al., 2004) and that blockade of sensory input results in reduced turnover of these cells (Zou et al., 2004). The continuous replacement of the granule cell population provides another model of competitive neuronal survival and differentiation. Many studies have demonstrated that odor deprivation leads to the reduced radial migration of neuroblasts (Saghateljan et al., 2004) and decreases the survival of newborn interneurons in the MOB (Frazier-Cierpial and Brunjes, 1989; Brunjes, 1994; Corotto et al., 1994). In contrast, an odor-enriched environment increases the total number of granule cells in rat pups (Rosselli-Austin and Williams, 1990) and the total number of newborn granule cells in adult mice (Rochefort et al., 2002). Supporting these findings, we found that deprivation specifically reduced the number of newborn granule cells and drastically altered their morphology. Dendritic length and spine density were reduced, respectively, by 31% and 45% following nostril occlusion. Since new granule cells massively contact mitral cells, and since previous electron microscopy studies demonstrated a 46% reduction in granule-to-mitral cell synapses following sensory deprivation (Benson et al., 1984), our data indicate that odor deprivation might exclusively affect the synaptic development of newborn granule cells, without altering the preexisting population. In agreement with this, our analyses of the resident population of granule cells clearly demonstrated that sensory deprivation fails to modify their morpho-functional properties, indicating that differences in either intrinsic properties or extrinsic (microenvironmental) signals of granule cells generated in distinct spatiotemporal windows underlie an exclusive role of sensory activity on the maturation of newborn cells.

Functional Consequences of a Reduced Number/Spine Density of Newborn Interneurons

A reduction in the spine density of newborn cells occurs in response to changing levels of sensory input, and this concomitantly decreases the frequency of mIPSCs impinging onto mitral cells. Since a direct correlation between the number of release sites/synapses and the frequency of neurotransmitter release has been clearly established in the CNS (Auger and Marty, 2000),

the reduced mIPSC frequency seen in deprived bulbs likely reflects the reduction in spine density. mIPSC amplitude was not affected, implying that sensory input does not alter postsynaptic GABA_A receptors. Similarly, intrinsic membrane properties as well as dendritic release of glutamate from mitral cells remained unaffected. These data, together with anatomical investigations of mitral cells (Benson et al., 1984; Matsutani and Yamamoto, 2000; but see Meisami and Safari, 1981), indicate that the overall level of sensory input is not required for the maintenance of the functional state of bulbar output neurons.

Whereas odor deprivation substantially reduced the frequency of mIPSCs, the increase in action potential-dependent GABA release from granule cells rescues the frequency of sIPSCs. Similarly, whereas only slightly reduced evoked inhibitory and excitatory dendrodendritic responses were observed in the occluded bulb in the presence of TTX, they were higher when action potential-dependent neurotransmitter release was intact. This suggests that a reduced spine density slightly affects the local inhibition of mitral cells, whereas the compensatory increase in the action potential-dependent GABA release upholds global inhibition.

Additionally, unaltered synchronization of mitral cells was observed following sensory deprivation. Thus, it is conceivable that, in addition to its dramatic effect on neurogenesis and spinogenesis, sensory deprivation activates other action potential-dependent homeostatic compensatory mechanisms that preserve the normal functioning of MOB circuitry. The most likely explanation for an elevated action potential-dependent release of GABA lies in the increase in granule cell excitability via a change in the activation threshold of the voltage-gated Na⁺ current. A similar mechanism for increased excitability was reported in other systems (Zhang and Linden, 2003), and theoretical models have suggested that neurons can maximize the information content of a stimulus response by adapting their firing rate (Stemmler and Koch, 1999). Interestingly, our experiments clearly established that only the newborn, but not the preexisting, granule cells were much more excitable. This suggests that the specific reduction in the spine density of newborn neurons was accompanied by a modification in the voltage dependency of their Na⁺ currents. This would favor the generation of action potentials and thus would compensate for the reduced tonic GABAergic output from the newborn cells. Such a homeostatic mechanism might take place if newborn granule cells receive appropriate information from their target cells (Zhang and Linden, 2003; Turrigiano and Nelson, 2004). Interestingly, an altered excitatory-inhibitory balance was observed in granule cells in the occluded bulb. However, these changes were subtle, and it is not clear whether they could be sufficient to trigger homeostatic mechanisms.

In addition, it should be noted that the spatial distribution of synaptic contacts impinging on newborn granule cells is likely to be remodeled in deprived bulbs. This might provide the required information to trigger homeostatic changes. Indeed, dendrites of newborn granule cells in the occluded bulb were found to be shorter. In control conditions, excitatory inputs received at the terminal dendritic field of granule cells

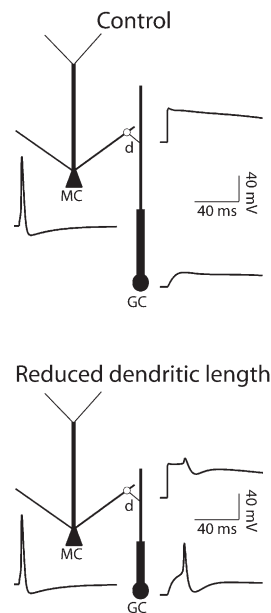


Figure 8. Reduced Dendritic Length of Newborn Granule Cells Changes Their Functional State

Schematic representation of the model under control conditions (top) and following odor deprivation (bottom). A granule cell (GC) in the odor-deprived bulb was modeled with a 40% reduction in the length of the dendrite. Traces below each model are the somatic membrane potential of the mitral cells (M), and the membrane potential of the terminal dendritic tips (d) and soma (GC) of the granule cell. Note the appearance of the somatic action potential in the granule cell following the reduction in the length of the dendrite.

rarely induce sufficient depolarization in the somatic compartment to generate Na^+ -dependent action potentials (Cang and Isaacson, 2003; Egger et al., 2003; Shepherd et al., 2004). However, due to the reduction in the dendrite length, and consequently in the electrotonic distance that dendritic signals should propagate to reach the cell soma, newborn granule cells in the occluded bulb might be more excitable. To assess this possibility, we modeled a 40% reduction in the length of newborn granule cell dendritic arborizations following sensory deprivation (Figure 8). As indicated in Figure 6G (left), a single action potential elicited in a mitral cell in a control bulb fails to induce sufficient depolarization of the somatic compartment of granule cells and thus does not trigger an action potential (Figure 8). When the length of the dendritic arborization was reduced by 40%, the EPSP-triggered depolarization was now able to reliably trigger action potentials (compare GC traces in Figure 8). This indicates that the same excitatory input impinging onto newborn granule cell dendrites differently affects their spike generation in control and odor-deprived bulbs and thus might be the required signal to trigger homeostatic changes. It should be also noted that this mechanism might serve only to trigger homeostatic plasticity in newborn granule cells and will not increase action potential-dependent GABA release on its own, since application of Kyn does not attenuate the increased excitability of newborn granule cells in the occluded bulb.

A long-term increase in the intrinsic excitability of visual cortical neurons following elevation of firing activity in these cells has been recently reported (Cudmore and Turrigiano, 2004). This increased excitability was accompanied by a decrease in the threshold current and voltage, without any changes in passive membrane properties. It has been widely suggested that spiking activity of cells might control different processes such as gene expression and phosphorylation of different proteins (Misonou et al., 2004). Intriguingly, it has been demonstrated that odor deprivation can influence the phosphorylation of different voltage-gated channels (Fadool et al., 2000), and phosphorylation of Na^+ channels may shift the voltage dependency of Na^+ current activation (Cantrell and Catterall, 2001), the experimental finding that we observed.

Alternatively, granule cells in the odor-deprived bulb may receive appropriate information via centrifugal pathways. It is well established that centrifugal fibers heavily contact granule cells (Shepherd et al., 2004) and that sensory deprivation markedly affect their organization. For instance, it has been shown that restriction of odor information increases the noradrenaline content (Brunjes et al., 1985; Guthrie et al., 1991; Wilson and Wood, 1992), and this could affect the functional state of granule cells. Whatever the exact nature of the signal is, our data demonstrate that a reduced spine density of newborn interneurons and a decreased frequency of mIPSCs following sensory deprivation are compensated for by an increased excitability of newborn granule cells.

Compensatory Responses to Odor Deprivation

While olfactory deprivation induces dramatic neuroanatomical and neurochemical alterations (Brunjes, 1994), the overall olfactory system remains fairly intact, even when olfactory deprivation starts at P1–P2 (Leon, 1998). For instance, while odor deprivation decreases the dopamine content of the MOB (Brunjes et al., 1985; Philpot et al., 1998), a higher density of dopamine D2 receptors counteracts this effect (Guthrie et al., 1991). Similarly, the reduction in size of the glomerular neuropil following occlusion (Meisami and Noushinfar, 1986) is compensated for by reorganizations in the synaptic distribution (Johnson et al., 1996). Normal olfactory responses of odor-deprived animals have even been demonstrated at the behavioral level (Stahl et al., 1990). These observations, together with our present report, suggest that a reduction in olfactory experience induces relatively little functional damage in spite of the reduction in both neurogenesis and tonic GABAergic inhibition. Altogether, our results demonstrate that the bulbar neuronal network detects sensory input perturbations to drive experience-dependent plasticity that preserves the normal functional state of the bulbar network.

Experimental Procedures

Animals and Surgical Procedures

All experiments were performed on Wistar rats obtained from Charles River (Chatillon sur Chalaronne, France). On P4–P5, unilateral naris occlusion via cauterization of either the right or the left naris was performed on cold-anesthetized rat pups (Meisami,

1976). All experimental procedures were in accordance with the Society for Neuroscience and European Union guidelines and were approved by our institutional animal care and utilization committees.

BrdU Labeling and Detection

To determine the quantity of newly generated cells, a DNA synthesis marker, BrdU was administered intraperitoneally (50 mg/kg of body weight). To assess neurogenesis (which includes cell proliferation, migration, differentiation, and survival) in the granule cell layer, one group ($n = 6$) received four BrdU injections (one every 2 hr) at P16 (i.e., 12 days after the unilateral nostril occlusion was performed) and were killed at P37. To assess proliferation in the SVZ, the other group ($n = 4$) received a single dose of BrdU at P37 and were sacrificed 4 hr after BrdU injection. Additionally, a single BrdU injection in P3 pups ($n = 3$) was used to analyze the number of newborn cells born locally in the MOB. From all groups, rats were given an overdose of sodium pentobarbital (100 mg/kg; Sanofi, Gentilly, France) and perfused transcardially with 4% PFA. Primary mouse anti-BrdU antibody (1:50; Euro-Diagnostica AB, Malmö, Sweden) was applied on free-floating 40 μm thick coronal sections that were pretreated with 0.2% triton and the DNA denaturing agent HCl (2 N; 30 min at room temperature). The number of BrdU profiles was determined by using the peroxidase method with biotinylated horse anti-mouse IgG antibody (1:50; Vector Laboratories, Inc., Burlingame, CA) and diaminobenzidine (0.05%) as a chromogen. To detect BrdU/NeuN double-labeled cells, the slices were first incubated with rat anti-BrdU (1:200; Accurate Scientific, Harlan Sera-lab, Loughborough, UK) and mouse anti-NeuN (1:200; Chemicon, Temecula, CA) primary antibodies and then with Alexa 568-labeled goat anti-rat IgG and Alexa 488-labeled goat anti-mouse IgG fluorescent secondary antibodies (Molecular Probes, Poortgebouw, Netherlands).

Stereotaxic Injections

GFP-encoded lentivirus was stereotactically injected to the ipsi- and contralateral SVZs, 15–18 days after unilateral nostril occlusion. The morphology and spine density of newborn neurons was assessed in the bulb 25 days after virus injection. Stereotaxic injections were performed using a Kopf stereotaxic apparatus (Harvard Apparatus, Les Ulis, France) at the following coordinates (relative to bregma): anteroposterior = 0, mediolateral = 1.6, dorsoventral = 3.0; and anteroposterior = 1.6, mediolateral = 1.5, dorsoventral = 3.5. To assess the morphology and spine density of the resident population of granule cells, Dil was injected into the MOB of P3 pups, and the cells were analyzed at P12, or alternatively, Dil was injected directly into P12 MOB slices.

Image Analysis and Quantification

To assess the number of newly generated neurons in the granule cell layer, BrdU-immunostained nuclei visualized through a 20 \times objective (BX51; Olympus, Hamburg, Germany) were counted for entire granule and periglomerular cell layers on every third section (120 μm apart). The number of BrdU profiles was then related to the areas of the two layers to evaluate the density of BrdU-positive cells. Immunofluorescent sections were analyzed using a Zeiss confocal microscope (Carl Zeiss S.A.S., Le Pecq, France). The percentage of BrdU/NeuN double-immunostained cells was obtained by analyzing BrdU $^{+}$ nuclei in the x-z and y-z orthogonal projections for the presence or absence of NeuN.

To analyze the morphology and spine density of newborn and preexisting neurons in control and odor-deprived bulbs, biphoton imaging of GFP-positive or spinning disk analysis of Dil-positive cells in 300 μm thick sections was performed. Biphoton imaging was performed using Axiovert 200M on a LSM510 Meta Zeiss microscope. A Titanium-Sapphire laser (Mira Verdi, Coherent, Santa Clara, CA) was used to excite GFP at 880–890 nm. Only cells located at least 30–60 μm from the surface of the slice were taken for analysis. Low-magnification (40 \times IR-Achroplan water immersion objective, 1.2 NA; digital zoom 0.7–1; 1 μm Z step) and high-magnification (40 \times ; digital zoom 5; 0.5 μm Z step) images of GFP-positive cells were taken to evaluate the general morphology and spine density of these cells. For Dil staining, images were taken with

spinning disk (Ultraview RS, Perkin Elmer) on Axiovert 200 with a 40 \times objective (Plan-Neofluar 1.3 NA). Images were deconvoluted using a maximum likelihood estimation method after calculation of the theoretical point spread function (PSF) (Huygens, Scientific Volume Imaging, Hilversum, Netherlands), while rendering of 3D data and measurements of dendritic length were performed with Imaris 3.2 (Bitplane) and Osirix (developed by Antoine Rosset, Geneva University Hospital) software.

Morphological data were compared between control and sensory-deprived bulbs using the Student's *t* test. All quantifications were performed blind to the experimental conditions.

Slice Preparation

Olfactory bulbs of P15 or P35–P40 rats were quickly removed and placed into cold oxygenated artificial cerebrospinal fluid (ACSF) containing 124 mM NaCl, 3 mM KCl, 2 mM CaCl_2 , 1.3 mM MgCl_2 , 25 mM NaHCO_3 , 1.25 mM NaH_2PO_4 , and 10 mM glucose. Horizontal slices (300 μm) were cut with a vibrating microslicer (DTK-1000, Dosaka, Japan) and kept in oxygenated ACSF at 32°C for 30 min.

Extracellular, Intracellular, and Whole-Cell Patch-Clamp Recordings

Recordings of LFPs were performed as previously described (Lagier et al., 2004). The conventional blind patch-clamp technique and visualized infrared microscopy (Olympus, BX51WI, Rungis, France) were used to record mitral and granule cells, respectively. Mitral cell recordings were performed with the help of an Axopatch-1D amplifier (Axon Instruments, Foster City, CA), whereas granule cells were recorded with an EPC9 patch-clamp amplifier (HEKA, Germany). Synaptic responses were analyzed with the MiniAnalysis program (Synaptosoft, Inc., Decatur, GA). Patch electrode resistance ranged from 4 to 6 M Ω when filled with an intracellular solution containing 134.5 mM CsCl, 10 mM HEPES, 0.2 mM EGTA, 8 mM NaCl, 2 mM ATP, 0.3 mM GTP, 0.2 mM AMP, and 10 mM glucose. For some granule cell recordings, CsCl was replaced with an equimolar concentration of KCl. To record evoked dendrodendritic reciprocal synaptic currents between mitral and granule cells, depolarizing pulses of 70 mV lasting 3, 5, 10, 25, or 50 ms were delivered to the recorded mitral cell. Na^{+} currents were recorded in Ca^{2+} -free ACSF and with a CsCl-based intracellular solution. K^{+} currents were recorded with a KCl-based intracellular solution and with 1 μM of TTX added to Ca^{2+} -free ACSF.

Computer Simulations

All simulations were carried out with the NEURON simulation program (Hines and Carnevale, 1997; v5.5) using its variable time step feature. The model and simulation files are available for public download under the ModelDB section of the Senselab database (<http://senselab.med.yale.edu/senselab/>). The model used in all simulations was composed of one mitral cell and one granule cell. The mitral cell was implemented as in a previous work (Migliore et al., 2005). The granule cell was modeled with a soma and a main radial dendrite (150 μm long) connected to a thinner, elongated (350 μm long) dendrite representing the medial and distal dendritic tree. To implement dendrodendritic coupling, a small oblique branch (5 μm length and 0.1 μm diameter) was connected at ~ 250 μm from the soma. Their terminal dendritic tips received AMPA and NMDA inputs with a peak conductance of 8 nS. The same kinetics were used for Na^{+} , fast (KA), and delayed rectified (KDR) K^{+} conductances in all cells. The mitral cell was modeled as a regularly firing cell, with Na^{+} , KA, and KDR conductances uniformly distributed over the entire dendritic tree (Bischofberger and Jonas, 1997). In the granule cell, Na^{+} channels were placed only in the soma, and KA was distributed throughout (Schoppa and Westbrook, 1999).

Acknowledgments

We are grateful to Matt Grubb and Kerren Murray for critical reading of the manuscript. Authors acknowledge support from the Pasteur Institute (GPH N°7 “Stem cells”), the Fondation pour la Recherche Médicale, the French Ministry of Research and Education (ACI Biologie du Développement et Physiologie Intégrative 2003

and Action 2003 "cellules souches"), and the Association Française contre les Myopathies. A.S. was supported by a postdoctoral fellowship from the Pasteur Institute and "Association Française contre les Myopathies."

Received: July 16, 2004

Revised: November 3, 2004

Accepted: February 7, 2005

Published: April 6, 2005

References

- Auger, C., and Marty, A. (2000). Quantal currents at single-site central synapses. *J. Physiol.* 526, 3–11.
- Baker, H., Cummings, D.M., Munger, S.D., Margolis, J.W., Franzen, L., Reed, R.R., and Margolis, F.L. (1999). Targeted deletion of a cyclic nucleotide-gated channel subunit (OCNC1): biochemical and morphological consequences in adult mice. *J. Neurosci.* 19, 9313–9321.
- Benson, T.E., Ryugo, D.K., and Hinds, J.W. (1984). Effects of sensory deprivation on the developing mouse olfactory system: a light and electron microscopic, morphometric analysis. *J. Neurosci.* 4, 638–653.
- Bischofberger, J., and Jonas, P. (1997). Action potential propagation into the presynaptic dendrites of rat mitral cells. *J. Physiol.* 504, 359–365.
- Brunjes, P.C. (1994). Unilateral naris closure and olfactory system development. *Brain Res. Brain Res. Rev.* 19, 146–160.
- Brunjes, P.C., Smith-Crafts, L.K., and McCarty, R. (1985). Unilateral odor deprivation: effects on the development of olfactory bulb catecholamines and behavior. *Brain Res.* 354, 1–6.
- Cang, J., and Isaacson, J.S. (2003). In vivo whole-cell recording of odor-evoked synaptic transmission in the rat olfactory bulb. *J. Neurosci.* 23, 4108–4116.
- Cantrell, A.R., and Catterall, W.A. (2001). Neuromodulation of Na⁺ channels: an unexpected form of cellular plasticity. *Nat. Rev. Neurosci.* 2, 397–407.
- Castillo, P.E., Carleton, A., Vincent, J.D., and Lledo, P.M. (1999). Multiple and opposing roles of cholinergic transmission in the main olfactory bulb. *J. Neurosci.* 19, 9180–9191.
- Chen, W.R., Xiong, W., and Shepherd, G.M. (2000). Analysis of relations between NMDA receptors and GABA release at olfactory bulb reciprocal synapses. *Neuron* 25, 625–633.
- Corotto, F.S., Henegar, J.R., and Maruniak, J.A. (1994). Odor deprivation leads to reduced neurogenesis and reduced neuronal survival in the olfactory bulb of the adult mouse. *Neuroscience* 61, 739–744.
- Cudmore, R.H., and Turrigiano, G.G. (2004). Long-term potentiation of intrinsic excitability in LV visual cortical neurons. *J. Neurophysiol.* 92, 341–348.
- Didier, A., Carleton, A., Bjaalie, J.G., Vincent, J.-D., Ottersen, O.P., Storm-Mathisen, J., and Lledo, P.-M. (2001). A dendrodendritic reciprocal synapse provides a recurrent excitatory connection in the olfactory bulb. *Proc. Natl. Acad. Sci. USA* 98, 6441–6446.
- Egger, V., Svoboda, K., and Mainen, Z.F. (2003). Mechanisms of lateral inhibition in the olfactory bulb: efficiency and modulation of spike-evoked calcium influx into granule cells. *J. Neurosci.* 23, 7551–7558.
- Fadool, D.A., Tucker, K., Phillips, J.J., and Simmen, J.A. (2000). Brain insulin receptor causes activity-dependent current suppression in the olfactory bulb through multiple phosphorylation of Kv1.3. *J. Neurophysiol.* 83, 2332–2348.
- Fiske, B.K., and Brunjes, P.C. (2001). Cell death in the developing and sensory-deprived rat olfactory bulb. *J. Comp. Neurol.* 437, 311–319.
- Frazier-Cierpial, L., and Brunjes, P.C. (1989). Early postnatal cellular proliferation and survival in the olfactory bulb and rostral migratory stream of normal and unilaterally odor-deprived rats. *J. Comp. Neurol.* 289, 481–492.
- Friedman, D., and Strowbridge, B.W. (2000). Functional role of NMDA autoreceptors in olfactory mitral cells. *J. Neurophysiol.* 84, 39–50.
- Friedman, D., and Strowbridge, B.W. (2003). Both electrical and chemical synapses mediate fast network oscillations in the olfactory bulb. *J. Neurophysiol.* 89, 2601–2610.
- Guthrie, K.M., Pullara, J.M., Marshall, J.F., and Leon, M. (1991). Olfactory deprivation increases dopamine D2 receptor density in the rat olfactory bulb. *Synapse* 8, 61–70.
- Halabisky, B., Friedman, D., Radojicic, M., and Strowbridge, B.W. (2000). Calcium influx through NMDA receptors directly evokes GABA release in olfactory bulb granule cells. *J. Neurosci.* 20, 5124–5134.
- Hinds, J.W. (1968). Autoradiographic study of histogenesis in the mouse olfactory bulb. I. Time of origin of neurons and neuroglia. *J. Comp. Neurol.* 134, 287–304.
- Hines, M.L., and Carnevale, N.T. (1997). The NEURON simulation environment. *Neural Comput.* 9, 1179–1209.
- Isaacson, J.S. (1999). Glutamate spillover mediates excitatory transmission in the rat olfactory bulb. *Neuron* 23, 377–384.
- Isaacson, J.S. (2001). Mechanisms governing dendritic gamma-aminobutyric acid (GABA) release in the rat olfactory bulb. *Proc. Natl. Acad. Sci. USA* 98, 337–342.
- Isaacson, J.S., and Strowbridge, B.W. (1998). Olfactory reciprocal synapses: dendritic signaling in the CNS. *Neuron* 4, 749–761.
- Johnson, B.A., Woo, C.C., Ninomiya-Tsui, K., and Leon, M. (1996). Synaptophysin-like immunoreactivity in the rat olfactory bulb during postnatal development and after restricted early olfactory experience. *Brain Res. Dev. Brain Res.* 92, 24–30.
- Kirschenbaum, B., Doetsch, F., Lois, C., and Alvarez-Buylla, A. (1999). Adult subventricular zone neuronal precursors continue to proliferate and migrate in the absence of the olfactory bulb. *J. Neurosci.* 19, 2171–2180.
- Lagier, S., Carleton, A., and Lledo, P.M. (2004). Interplay between local GABAergic interneurons and relay neurons generates gamma oscillations in the rat olfactory bulb. *J. Neurosci.* 24, 4382–4392.
- Laurent, G., Stopfer, M., Friedrich, R.W., Rabinovich, M.I., Volkovskii, A., and Abarbanel, H.D. (2001). Odor encoding as an active, dynamical process: experiments, computation, and theory. *Annu. Rev. Neurosci.* 24, 263–297.
- Leon, M. (1998). Compensatory responses to early olfactory restriction. *Ann. N Y Acad. Sci.* 855, 104–108.
- Lin, D.M., Wang, F., Lowe, G., Gold, G.H., Axel, R., Ngai, J., and Brunet, L. (2000). Formation of precise connections in the olfactory bulb occurs in the absence of odorant-evoked neuronal activity. *Neuron* 26, 69–80.
- Lledo, P.M., and Gheusi, G. (2003). Olfactory processing in a changing brain. *Neuroreport* 14, 1655–1663.
- Lledo, P.M., Saghatelian, A., and Lemasson, M. (2004). Inhibitory interneurons in the olfactory bulb: from development to function. *Neuroscientist* 10, 292–303.
- Lois, C., and Alvarez-Buylla, A. (1994). Long-distance neuronal migration in the adult mammalian brain. *Science* 264, 1145–1148.
- Luskin, M.B. (1993). Restricted proliferation and migration of postnatally generated neurons derived from the forebrain subventricular zone. *Neuron* 11, 173–189.
- Matsutani, S., and Yamamoto, N. (2000). Differentiation of mitral cell dendrites in the developing main olfactory bulbs of normal and naris-occluded rats. *J. Comp. Neurol.* 418, 402–410.
- Meisami, E. (1976). Effects of olfactory deprivation on postnatal growth of the rat olfactory bulb utilizing a new method for production of neonatal unilateral anosmia. *Brain Res.* 107, 437–444.
- Meisami, E., and Noshinifar, E. (1986). Early olfactory deprivation and the mitral cells of the olfactory bulb: a Golgi study. *Int. J. Dev. Neurosci.* 4, 431–444.
- Meisami, E., and Safari, L. (1981). A quantitative study of the effects of early unilateral olfactory deprivation on the number and distribu-

- p>tion of mitral and tufted cells and of glomeruli in the rat olfactory bulb.
- Brain Res.*
- 221, 81–107.
- Migliore, M., Hines, M.L., and Shepherd, G.M. (2005). The role of distal dendritic gap junctions in synchronization of mitral cell axonal output. *J. Comput. Neurosci.* 18, 151–161.
- Misonou, H., Mohapatra, D.P., Park, E.W., Leung, V., Zhen, D., Misonou, K., Anderson, A.E., and Trimmer, J.S. (2004). Regulation of ion channel localization and phosphorylation by neuronal activity. *Nat. Neurosci.* 7, 711–718.
- Najbauer, J., and Leon, M. (1995). Olfactory experience modulated apoptosis in the developing olfactory bulb. *Brain Res.* 674, 245–251.
- Nakajima, T., Murabayashi, C., Ogawa, K., and Taniguchi, K. (1998). Immunoreactivity of protein gene product 9.5 (PGP 9.5) in the developing hamster olfactory bulb. *Anat. Rec.* 250, 238–244.
- Petreaanu, L., and Alvarez-Buylla, A. (2002). Maturation and death of adult-born olfactory bulb granule neurons: role of olfaction. *J. Neurosci.* 22, 6106–6113.
- Philpot, B.D., Men, D., McCarty, R., and Brunjes, P.C. (1998). Activity-dependent regulation of dopamine content in the olfactory bulbs of naris-occluded rats. *Neuroscience* 85, 969–977.
- Price, J.L., and Powell, T.P.S. (1970). The morphology of granule cells within the olfactory bulb. *J. Cell Sci.* 7, 91–123.
- Rocheffort, C., Gheusi, G., Vincent, J.-D., and Lledo, P.-M. (2002). Enriched odor exposure increases the number of newborn neurons in the adult olfactory bulb and improves odor memory. *J. Neurosci.* 22, 2679–2689.
- Rosselli-Austin, L., and Williams, J. (1990). Enriched neonatal odor exposure leads to increased numbers of olfactory bulb mitral and granule cells. *Brain Res. Dev. Brain Res.* 51, 135–137.
- Saghatelian, A., Carleton, A., Lagier, S., de Chevigny, A., and Lledo, P.M. (2003). Local neurons play key roles in the mammalian olfactory bulb. *J. Physiol. (Paris)* 97, 517–528.
- Saghatelian, A., de Chevigny, A., Schachner, M., and Lledo, P.-M. (2004). Tenascin-R mediates activity-dependent recruitment of neuroblasts in the adult mouse forebrain. *Nat. Neurosci.* 7, 347–356.
- Salin, P.A., Lledo, P.-M., Vincent, J.-D., and Charkpak, S. (2001). Dendritic glutamate autoreceptors modulate signal processing in rat mitral cells. *J. Neurophysiol.* 85, 1275–1282.
- Schoppa, N.E., and Westbrook, G.L. (1999). Regulation of synaptic timing in the olfactory bulb by an A-type potassium current. *Nat. Neurosci.* 2, 1106–1113.
- Schoppa, N.E., Kinzie, J.M., Sahara, Y., Segerson, T.P., and Westbrook, G.L. (1998). Dendrodendritic inhibition in the olfactory bulb is driven by NMDA receptors. *J. Neurosci.* 18, 6790–6802.
- Schrader, L.A., Anderson, A.E., Varga, A.W., Levy, M., and Sweatt, J.D. (2002). The other half of Hebb: K⁺ channels and the regulation of neuronal excitability in the hippocampus. *Mol. Neurobiol.* 25, 51–66.
- Shepherd, G.M., Chen, R.C., and Greer, C.A. (2004). Olfactory bulb. In *The Synaptic Organization of the Brain*, G.M. Shepherd, ed. (New York: Oxford), pp. 165–216.
- Stahl, B., Distel, H., and Hudson, R. (1990). Effects of reversible nare occlusion on the development of the olfactory epithelium in the rabbit nasal septum. *Cell Tissue Res.* 259, 275–281.
- Stemmler, M., and Koch, C. (1999). How voltage-dependent conductances can adapt to maximize the information encoded by neuronal firing rate. *Nat. Neurosci.* 2, 521–527.
- Turrigiano, G.G., and Nelson, S.B. (2004). Homeostatic plasticity in the developing nervous system. *Nat. Rev. Neurosci.* 5, 97–107.
- Watt, W.C., Sakano, H., Lee, Z.Y., Reusch, J.E., Trinh, K., and Storm, D.R. (2004). Odorant stimulation enhances survival of olfactory sensory neurons via MAPK and CREB. *Neuron* 41, 955–967.
- Wilson, D.A. (1995). NMDA receptors mediate expression of one form of functional plasticity induced by olfactory deprivation. *Brain Res.* 677, 238–242.
- Wilson, D.A., and Wood, J.G. (1992). Functional consequences of unilateral olfactory deprivation: time-course and age sensitivity. *Neuroscience* 49, 183–192.
- Wilson, D.A., Guthrie, K.M., and Leon, M. (1990). Modification of olfactory bulb synaptic inhibition by early unilateral olfactory deprivation. *Neurosci. Lett.* 116, 250–256.
- Winner, B., Cooper-Kuhn, C.M., Aigner, R., Winkler, J., and Kuhn, H.G. (2002). Long-term survival and cell death of newly generated neurons in the adult rat olfactory bulb. *Eur. J. Neurosci.* 16, 1681–1689.
- Zhang, W., and Linden, D.J. (2003). The other side of the engram: experience-driven changes in neuronal intrinsic excitability. *Nat. Rev. Neurosci.* 4, 885–900.
- Zhao, H., and Reed, R.R. (2001). X inactivation of the OCNC1 channel gene reveals a role for activity-dependent competition in the olfactory system. *Cell* 104, 651–660.
- Zou, D.J., Feinstein, P., Rivers, A.L., Mathews, G.A., Kim, A., Greer, C.A., Mombaerts, P., and Firestein, S. (2004). Postnatal refinement of peripheral olfactory projections. *Science* 304, 1976–1979.